Adaptive Radial Basis Function Artificial Neural Network Control for Two-Flexible-Link Robots

Francis Kunzi Tekweme
Department of Mechanical and Industrial Engineering Technology
University of Johannesburg
Johannesburg, Republic of South Africa
ftekweme@uj.ac.za

Abstract

The focus of this paper is the use of an Adaptive Radial Basis Function Artificial Neural Network (ARBFANN) for the control of Two-Flexible-Link Robots (TFLR). Flexible links are modeled as Bernoulli beams. The Assumed Mode Method (AMM) together with the Lagrangian approach is used to derive the closed-form dynamic. Two modes are considered for each link. Singular perturbation method is used to derive a composite control for the TFLR. A stable robust two-time scale controller without any data for modeling is developed. The slow subsystem is controlled by an ARBFANN based on global approximation while the Linear Quadratic Regulator (LQR) controller stabilizes the fast subsystem and guarantee the closed-loop stability. The ARBFANN with a sliding mode robust term is trained on-line to approximate unknown nonlinear system dynamics, suppress errors in the modeling of neural network and, guarantee closed-loop stability. To verify the validity of the proposed control strategy, simulation results are included.

Keywords

Radial basis function, Artificial neural network, flexible links, singular perturbations and, assumed modes.

1. Introduction

Most studies involving the AMM consider the simplified orthogonality conditions to derive the finite-dimensional dynamic models of the multilink flexible robots (De Luca and Siciliano 1991, Subhudi and Morris 2001, Subhudi and Morris 2002). In those situations where the simplified orthogonality relations are used for TFLR, the diagonal block matrix relative to shoulder deflections elements depend on the assumed mode spatial shapes of shoulder link and their spatial derivatives. However, some previous studies considered complete orthogonality relations and their companions (Tekweme and Nel 2016, Tekweme 2018a, 2018b, 2018c). The use of the complete orthogonality relations and their companions results in simplified diagonal matrix blocks relative to shoulder link and elbow link (Tekweme and Nel 2016). In this regard, not only the dynamic model accuracy is improved but also the computational burden is reduced as far as the partition of the dynamics of a TFLR is concerned. Adaptive neural network control of a TLFR based on local model approximation using singular perturbation was proposed by Gee et al. (1997). They considered the assumed modes with one element for each link. However, they observed that a more accurate model can be derived using more than one element and the matrix gain for the fast subsystem was computed for the final joint configuration. Mehrdad et al. (1997) and Moallem et al. (1996) derived a two-scale control system for multilink robots with the singular perturbation technique. In their paper, a two-link planar robot manipulator built from a rigid shoulder link and a flexible elbow link was considered. Although numerous research based on neural networks without prior knowledge of robot dynamics, Liu (2013) observes that the knowledge of the dynamics of the robots can't be completely discarded. A robot neural network control designed without prior knowledge of the dynamics of the robots requires a huge number of nodes and considerable time is required for the controller to be trained (Rahimi and Nazemizadeh 2014).

This paper's target is to replace the nonlinear robot function with the neural network, track each joint trajectory with good robustness properties, and stabilize the fast variables. This paper is divided into sections. Section 1 deals with the introduction. In section 2, natural modes for the TLFR are normalized using the generalized orthonormality relations, instead of simplified one, on which the majority of studies are focused. And the TFLR closed-form

dynamics are presented. In section 3, the full dynamics of the TLFR is resolved into fast and slow subsystems using the singular perturbation technique. The ARBFANN control approach in Liu (2013) has been extended for the case of the slow subsystem control and the LQR design has been used to design the optimal control for the fast subsystem control. In section 4, numerical simulation results are presented. Finally, the conclusion is dealt with in section 5.

2. Two-Flexible-Link Robot Dynamics

The dynamic model of the two-flexible-link robot can be derived using Lagrange's equation together with the AMM. For convenience, natural modes for flexible links are normalized using the generalized orthonormality relations expressed as (Tekweme and Nel 2016)

$$\int_0^{l_i} \phi_{ij}(x_i)\rho_i\phi_{ik}(x_i)dx_i + \phi_{ij}(x_i)M_{Li}\phi_{ik}(x_i)\Big|_{x_i=l_i} + \frac{d\phi_{ij}(x_i)}{dx_i}J_{Li}\frac{d\phi_{ik}(x_i)}{dx_i}\Big|_{x_i=l_i} + (MD)_i\frac{d[\phi_{ij}(x_i)\phi_{ik}(x_i)]}{dx_i}\Big|_{x_i=l_i} = \begin{cases} 0 & j \neq k \\ P_i & j = k \end{cases} \quad (1)$$

where x_i is the distance from hub i along link i, $\phi_{ij}(x_i)$ is the jth assumed spatial mode shape of link i, ρ_i is the mass per unit length of link i, M_{Li} is the actual mass at the distal end of link i, J_{Li} is the actual moment of inertia at the distal end of link i, $(MD)_i$ is the contribution of masses non-collocated at the distal end of link i, and P_i is the scale factor (i.e., normalizing constant).
The dimensionless expressions of the generalized orthonormality relations were derived in Tekweme (2018c).
The closed-form dynamic model of TFLR derived from Lagrange's equation together with the assumed spatial modes normalized by (1) can be written as follows

$$\begin{bmatrix} M_{\theta\theta} & M_{\theta\delta} \\ M_{\delta\theta} & M_{\delta\delta} \end{bmatrix}\begin{bmatrix} \ddot{\theta} \\ \ddot{\delta} \end{bmatrix} + \begin{bmatrix} C_{\theta\theta} & C_{\theta\delta} \\ C_{\delta\theta} & C_{\delta\delta} \end{bmatrix}\begin{bmatrix} \dot{\theta} \\ \dot{\delta} \end{bmatrix} + \begin{bmatrix} 0 & 0 \\ 0 & K_{\delta\delta} \end{bmatrix}\begin{bmatrix} \theta \\ \delta \end{bmatrix} = \begin{bmatrix} \tau \\ 0 \end{bmatrix} \quad (2)$$

where
$\theta = (\theta_1, \theta_2)^T$ is the vector of joint angles;
$\delta = (\delta_{11}, \delta_{12}, \delta_{21}, \delta_{22})^T$ is the vector of links deflection variables;
$M_{\theta\theta}, M_{\theta\delta}, M_{\delta\theta}$ and $M_{\delta\delta}$ are the blocks of the inertia matrix;
$C_{\theta\theta}, C_{\theta\delta}, C_{\delta\theta}$ and $C_{\delta\delta}$ are the blocks of the Coriolis/ centripetal matrix;
$K_{\delta\delta}$ is the positive definite stiffness matrix; and
τ is the vector torque input.

In equation (2), when $P_i = m_i$ the block matrices may be written as [Tekweme and Nel 2016]

$$M_{\delta\delta} = \begin{bmatrix} m_1 & 0 & M_{35} & M_{36} \\ 0 & m_1 & M_{45} & M_{46} \\ M_{35} & M_{45} & m_2 & 0 \\ M_{36} & M_{46} & 0 & m_2 \end{bmatrix} \text{ and } K_{\delta\delta} = \begin{bmatrix} m_1\omega_{11}^2 & 0 & 0 & 0 \\ 0 & m_1\omega_{12}^2 & 0 & 0 \\ 0 & 0 & m_2\omega_{21}^2 & 0 \\ 0 & 0 & 0 & m_2\omega_{22}^2 \end{bmatrix} \quad (3)$$

where m_i is the mass of link i and i=1,2. Link 1 represents the shoulder link and link 2 represents the elbow link.

It can be observed that the diagonal blocks relative to link 1 and link 2 deflections reduce to diagonal matrices, which alleviates the computational burden. The inertia matrix and its inverse can be written as

$$M = \begin{bmatrix} M_{\theta\theta} & M_{\theta\delta} \\ M_{\delta\theta} & M_{\delta\delta} \end{bmatrix} \quad and \quad M^{-1} = \begin{bmatrix} H_{\theta\theta} & H_{\theta\delta} \\ H_{\delta\theta} & H_{\delta\delta} \end{bmatrix} \quad (4)$$

Substituting (4) into (2) yields

$$\ddot{\theta} = -W_{\theta\theta}\dot{\theta} - W_{\theta\delta}\dot{\delta} - K_{\theta\delta}^{*}\delta + H_{\theta\theta}\tau \quad (5)$$

$$\ddot{\delta} = -W_{\delta\theta}\dot{\theta} - W_{\delta\delta}\dot{\delta} - K_{\delta\delta}^{*}\delta + H_{\delta\theta}\tau \quad (6)$$

where

$$W_{\theta\theta} = H_{\theta\theta}C_{\theta\theta} + H_{\theta\delta}C_{\delta\theta} \quad (7)$$

$$W_{\theta\delta} = H_{\theta\theta}C_{\theta\delta} + H_{\theta\delta}C_{\delta\delta} \quad (8)$$

$$W_{\delta\theta} = H_{\delta\theta}C_{\theta\theta} + H_{\delta\delta}C_{\delta\theta} \quad (9)$$

$$W_{\delta\delta} = H_{\delta\theta}C_{\theta\delta} + H_{\delta\delta}C_{\delta\delta} \quad (10)$$

$$K^{*}_{\theta\delta} = H_{\theta\delta}K_{\delta\delta} \quad (11)$$

$$K^{*}_{\delta\delta} = H_{\delta\delta}K_{\delta\delta} \quad (12)$$

3. Two-Time Scale Controller Design

It can be assumed that the spectra of the rigid joints motions described in equation (2) are separated by a considerable margin from the spectra of the flexible link deflections (Siciliano and Book 1988), which reveals the simultaneous existence of high-frequency and low-frequency oscillations (Cai et al. 2017). To expatiate the existence of the high-frequencies oscillations in equation (2), Siciliano and Book (1988) introduced elastic forces as new state variables as follows

$$\xi = K_{\delta\delta min}\delta \quad or \quad \delta = \varepsilon^2\xi \quad (13)$$

where $K_{\delta\delta min}$ is the smallest stiffness constant of the stiffness matrix $K_{\delta\delta}$ and $\varepsilon^2 = \frac{1}{K_{\delta\delta min}}$.

Under the assumption that the stiffness of the links are relatively large, $K_{\delta\delta}$ can be written as follows (Zhu et al. 1994),

$$K_{\delta\delta} = K_{\delta\delta min}\widetilde{K}_{\delta\delta} \quad (14)$$

where $\widetilde{K}_{\delta\delta}$ is independent of the stiffness.

Siciliano et al. (1992) observed that the rigid body dynamics can be separated from flexible dynamics on condition that $\frac{1}{K_{\delta\delta min}} << 1$ so that the limit $\varepsilon^2 \to 0$ corresponds to an equivalent rigid manipulator.

Tekweme (2018c) showed that the behavior of the flexible robot depends on the dimensionless stiffness of the joint, which is defined as the joint spring stiffness to the link flexural rigidity ratio.

Using the new state variables, (5) and (6) can be expressed as follows

$$\ddot{\theta} = -W_{\theta\theta}\dot{\theta} - \varepsilon^2 W_{\theta\delta}\,\dot{\xi} - H_{\theta\delta}\widetilde{K}_{\delta\delta}\,\xi + H_{\theta\theta}\tau \quad (15)$$

$$\varepsilon^2\ddot{\xi} = -W_{\delta\theta}\dot{\theta} - \varepsilon^2 W_{\delta\delta}\dot{\xi} - H_{\delta\delta}\widetilde{K}_{\delta\delta}\xi + H_{\delta\theta}\tau \quad (16)$$

where (15) and (16) represent the high-order systems where the parameter ε represents small time constants (Kokotović and Haddad 1975).

To avoid the challenges facing the higher-order systems in the design of time-optimal control, the full order system will be resolved into two reduced-order subsystems: a slow subsystem and a fast subsystem (Siciliano and Book 1988).

3.1. Slow Subsystem Control

The slow subsystem control is designed to track the joint desired trajectory. To design the slow subsystem control, it can be assumed that the contributions of the deflections to the inertia matrix is negligible, i.e. ε = 0 and the terms involving the products of δ *or* $\dot{\delta}$ with δ *or* $\dot{\delta}$ are negligible (Siciliano and Book 1988).

Setting ε = 0, the full order systems (15) and (16) reduce to

$$\ddot{\bar{\theta}} = -\overline{W}_{\theta\theta}\dot{\bar{\theta}} - \overline{H}_{\theta\delta}\,\widetilde{K}_{\delta\delta}\,\bar{\xi} + \overline{H}_{\theta\theta}\bar{\tau} \quad (17)$$

$$0 = -\bar{W}_{\delta\theta}\dot{\bar{\theta}} - \bar{H}_{\delta\delta}\bar{K}_{\delta\delta}\bar{\xi} + \bar{H}_{\delta\theta}\bar{\tau} \tag{18}$$

where the overbar designates the evaluation of the robot parameters with $\varepsilon = 0$.
Solving for $\bar{\xi}$ using the transcendental equation (18) yields

$$\bar{\xi} = \bar{K}_{\delta\delta}^{-1}\bar{H}_{\delta\delta}^{-1}\left(-\bar{W}_{\delta\theta}\dot{\bar{\theta}} + \bar{H}_{\delta\theta}\bar{\tau}\right) \tag{19}$$

Note that $\bar{\xi}$ is called the slow manifold.

Substituting (19) into (17) yields

$$\bar{M}_{\theta\theta}\ddot{\bar{\theta}} + \bar{C}_{\theta\theta}\dot{\bar{\theta}} = \bar{\tau} \tag{20}$$

Considering the desired angle vector $\theta_d(t)$, the tracking error vector can be defined as follows

$$e = \theta_d(t) - \bar{\theta}(t) \text{ and } \dot{e} = \dot{\theta}_d(t) - \dot{\bar{\theta}}(t) \tag{21}$$

The filtered tracking error r is defined as follows

$$r = \dot{e} + \Lambda e \tag{22}$$

where Λ is a symmetric positive definite matrix.

Substituting (21) and (22) into (20), the reduced-order slow subsystem can be expressed as (Lewis et al. 1995),

$$\bar{M}_{\theta\theta}\dot{r} = -\bar{C}_{\theta\theta}r - \bar{\tau} + f(x) \tag{23}$$

where the nonlinear robot function that contains all the slow subsystem modeling information is

$$f(x) = \bar{M}_{\theta\theta}\left(\ddot{\theta}_d + \Lambda\dot{e}\right) + \bar{C}_{\theta\theta}\left(\dot{\theta}_d + \Lambda e\right) \tag{24}$$

In this paper, the ARBFANN is used for global approximation of the nonlinear robot function that contains all the subsystem modeling information.
The structure of the RBF neural network adapted from Liu (2013) is shown in Figure 1.

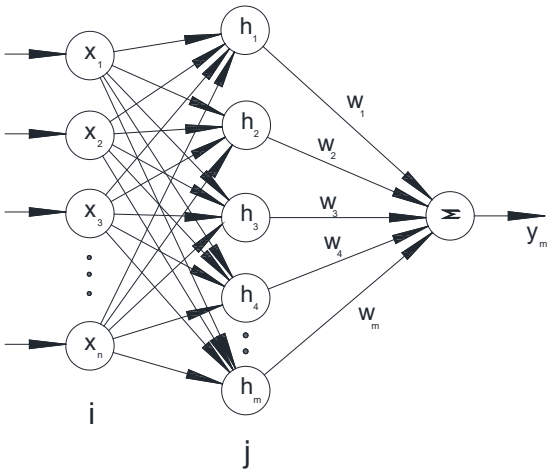

Figure 1: RBF Neural network structure

The algorithm of the RBF is expressed as follows (Liu 2013)

$$h_i = g\left(\frac{\|x - c_i\|^2}{b_i^2}\right) \quad i = 1,2, \ldots\ldots, n. \tag{25}$$

$$y = w^T h(x) \tag{26}$$

where x is the input vector, w is the neural network weight value, $h=[h_1, h_2, \ldots\ldots, h_n]$ is the Gaussian function output, c_i represents the centre point coordinate of the Gaussian function of the neural net i and b_i.
The ARBFANN controller in (Lewis et al. 1995) is extended to TLFR as follows,

$$\bar{\tau} = \hat{f}(x) + k_v r - v \tag{27}$$

$$\hat{f}(x) = \hat{w}^T h(x) \tag{28}$$

where θ_d is the ideal position (angle), $k_v > 0$ is the gain matrix, v is the robustness term, $\hat{w}$ is the estimation value of w and $\hat{f}(x)$ is the estimation of $f(x)$.
where the adaptive law is given by

$$\dot{\hat{w}} = \Gamma h r^T \tag{29}$$

and $\Gamma = \Gamma^T > 0$ is any constant matrix.

Concerning the slow subsystem, the following approximations apply (Borne et al. 1992)

$$for\ t \in [t_0, +\infty[: \theta(t) \approx \bar{\theta}(t)\ and\ \dot{\theta}(t) \approx \dot{\bar{\theta}}(t) \tag{30}$$

where t_0 is the initial time

3.2. Fast Subsystem Control

The fast subsystem is derived under the assumption that the variations of slow subsystem variables are relatively small as compared to the variations of fast subsystem variables in the boundary layers (Siciliano and Book 1988). Considering the fast subsystem state variables change around the equilibrium trajectory $\zeta_1 = \xi - \bar{\xi}$ and in an analogous way the control $\tau_F = \tau - \bar{\tau}$ (Bruno and Book 1988),

the new states for the design of the fast subsystem are defined as follows

$$\zeta_1 = \xi - \bar{\xi} \quad \text{and} \quad \zeta_2 = \varepsilon\dot{\xi} \tag{31}$$

where ζ_1 is the off-manifold error function (Zhu et al. 1994).

Differentiating ζ_1 and ζ_2 under the assumption that the slow manifold does not vary in the boundary layer, we obtain

$$\varepsilon\dot{\zeta}_1 = \zeta_2 \tag{32}$$

$$\varepsilon\dot{\zeta}_2 = \varepsilon^2\ddot{\xi} \tag{33}$$

Considering the fast time scale $T = \frac{t}{\varepsilon}$ and (16), equations (32) and (33) result in

$$\frac{d\zeta_1}{dT} = \zeta_2 \tag{34}$$

$$\frac{d\zeta_2}{dT} = -W_{\theta\theta}\ddot{\theta} - \varepsilon^2 W_{\theta\theta}\ddot{\xi} - H_{\theta\theta}\bar{K}_{\theta\theta}(\zeta_1 + \bar{\xi}) + H_{\theta\theta}(\bar{\tau} + \tau_F) \tag{35}$$

Setting ε=0, the fast system can be written as (Lewis et al. 1998)

$$\frac{d}{dT}\begin{bmatrix}\zeta_1\\ \zeta_2\end{bmatrix}=\begin{bmatrix}0 & I\\ -\bar{H}_{\delta\delta}\bar{K}_{\delta\delta} & 0\end{bmatrix}\begin{bmatrix}\zeta_1\\ \zeta_2\end{bmatrix}+\begin{bmatrix}0\\ \bar{H}_{\delta\theta}\end{bmatrix}\tau_F \tag{36}$$

The Linear Quadratic Regulator (LQR) approach will be used to determine the gains of the PD controller (Lewis et al. 1995)

$$\tau_F = -K_{PF}\zeta_1 - K_{DF}\zeta_2 \tag{37}$$

3.3 Composite controls design

The composite controller for the full system (2) is obtained from (20) and (37) as follows (Chow and Kokotovic 1978):

$$\tau = \bar{\tau} + \tau_F \tag{38}$$

4. Simulation results

Numerical simulations are performed in this section to validate the efficacy of the control strategy outlined in this paper. The flexible links are modeled as Bernoulli beams with two flexible modes. The clamped-mass boundary conditions are considered to derive the mode shapes of a TFLR. Two modes are considered for each link. The two-flexible-link robot data are shown in Table 1.

Table 1 TFLR physical parameter

Symbol	Parameter	Value	Unit
$m_1 = m_2$	Link mass	0.09	kg
m_{h2}	Hub 2 mass	0.98	kg
m_p	Payload mass	0.09	kg
$l_1 = l_2$	Link length	0.5	m
$b = b_1 = b_2$	Link thickness	0.0015	m
$h_t = h_{t1} = h_{t2}$	Link height	0.048	m
E	Link modulus of elasticity	69	GPa
$J_{h1} = J_{h2}$	Hub moment of inertia	0.102	kgm^2
J_p	Payload moment of inertia	0.00048	kgm^2
$P_1 = P_2$	Normalizing scale factor for link	0.09	kg

In this paper, the clamped-mass boundary conditions are considered. The spatial mode shapes for the two-flexible-link robot are shown in Figures 2 and 3.

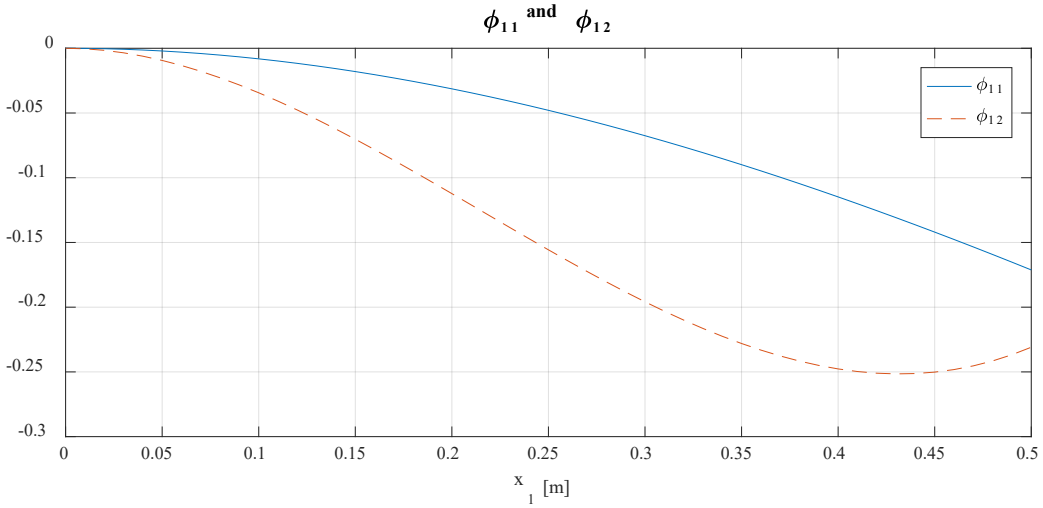

Figure 2: Spatial eigenfunctions for link 1

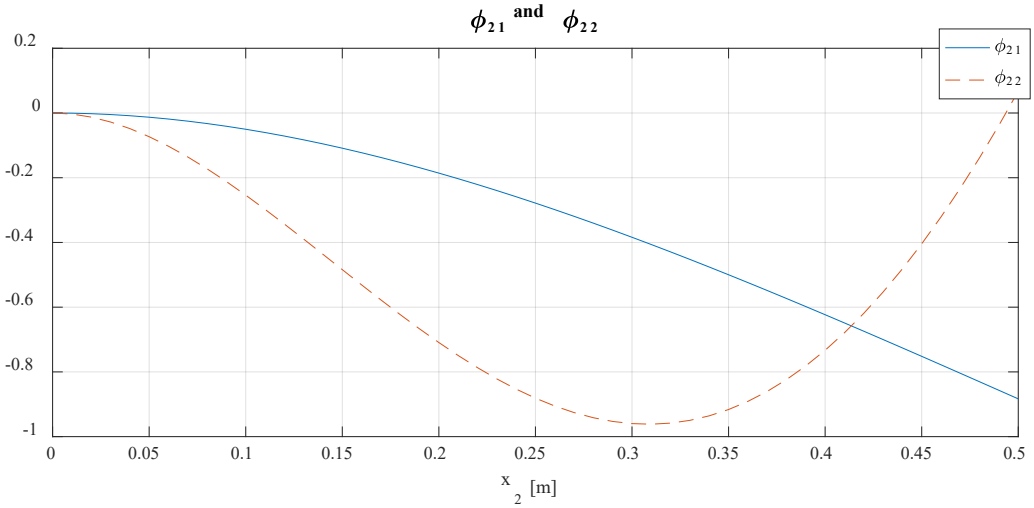

Figure 3: Spatial eigenfunctions for link 2

The desired angular position for each joint is given by

$$\theta_d(t) = \frac{5}{3}\left(\frac{\pi}{t_f^3}\right)t^3 - \frac{5}{2}\left(\frac{\pi}{t_f^4}\right)t^4 + \left(\frac{\pi}{t_f^5}\right)t^5 \tag{38}$$

where t_f is the time for the desired angular trajectory to reach the final position.
To assess the efficacy of the adaptation ability of the control system, a slight initial error is assigned to the actual trajectory. To this end, the initial actual position and speed are $\theta(0) = [0.6 \quad 0.6]^T$ deg and $\dot{\theta}(0) = [0 \quad 0]^T$ deg /s respectively.
For the adaptive radial basis function artificial neural network, the structure 2-7-1 is adopted and the input vector is $[e, \dot{e}\,]$. The parameter of the Gaussian function c_i and b_i are chosen as follows (Liu 2013):
$[-1.5 \; -1.0 \; -0.5 \; 0 \; 0.5 \; 1.0 \; 1.5] \quad and \quad 10$.
The initial weight for the NN is zero. The LQR is designed to stabilize the fast subsystem is based on the final configuration of each joint (Ge et al. 1997). MATLAB was used to derive the gains for the slow subsystem using the following weights:

$$R = diag[0.8 \quad 1] \quad \text{and} \quad Q = diag[0 \;\; 0 \;\; 0 \;\; 0 \;\; 0.0005 \;\; 0.005 \;\; 0.025 \;\; 0.03] \tag{39}$$

The following gains are obtained

$$K_{PF} = \begin{bmatrix} 13.21 \times 10^{-5} & -20.76 \times 10^{-3} & 85.57 \times 10^{-3} & -51.52 \times 10^{-2} \\ -87.68 \times 10^{-5} & -58.54 \times 10^{-3} & -19.65 \times 10^{-2} & 10.17 \times 10^{0} \end{bmatrix} \quad (40)$$

$$K_{DF} = \begin{bmatrix} 16.96 \times 10^{-3} & 23.58 \times 10^{-3} & -19.62 \times 10^{-3} & 16.98 \times 10^{-3} \\ 16.65 \times 10^{-3} & -57.89 \times 10^{-3} & 16.07 \times 10^{-2} & -15.21 \times 10^{-2} \end{bmatrix} \quad (41)$$

Simulations have been carried out via MATLAB. To test the robustness of the proposed control strategy in the presence of disturbances, slight initial joint angle tracking errors are incorporated deliberately, i.e.,

$$\theta_1(0) = 4 \ deg \ ; \quad \theta_2(0) = 4 \ deg \quad (42)$$

Figures 4 and 5 show the joint position tracking performances of the TFLR. It can be noticed that there is a significant initial tracking error that vanishes in less than 1 second as it can also be observed in Figure 6. Figures 7 and 8 show the tracking performance of the end-point of the TFLR. , it can be observed that the tip transverse and longitudinal displacement tracking performances are good. The contributions of the control for the slow subsystem to the performance of components of the subsystems to the performances are displayed in Figure 9. It can be noticed that the pure ARBFANN control applied to the full order system guarantees the tracking of the desired trajectories with acceptable performance. The inclusion of the optimal control in the composite control increases the control effectiveness.

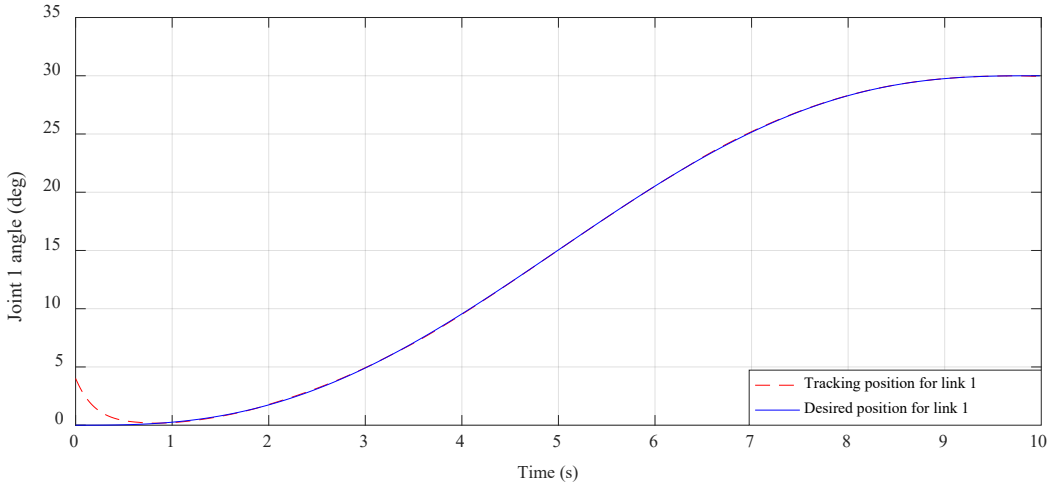

Figure 4. The tracking position and desired position for link 1.

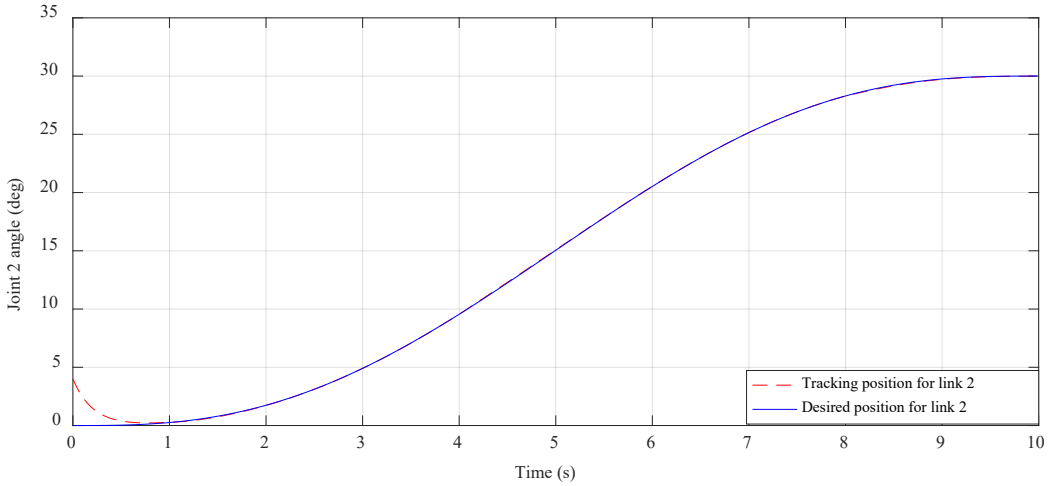

Figure 5. The tracking position and the desired position for link 2.

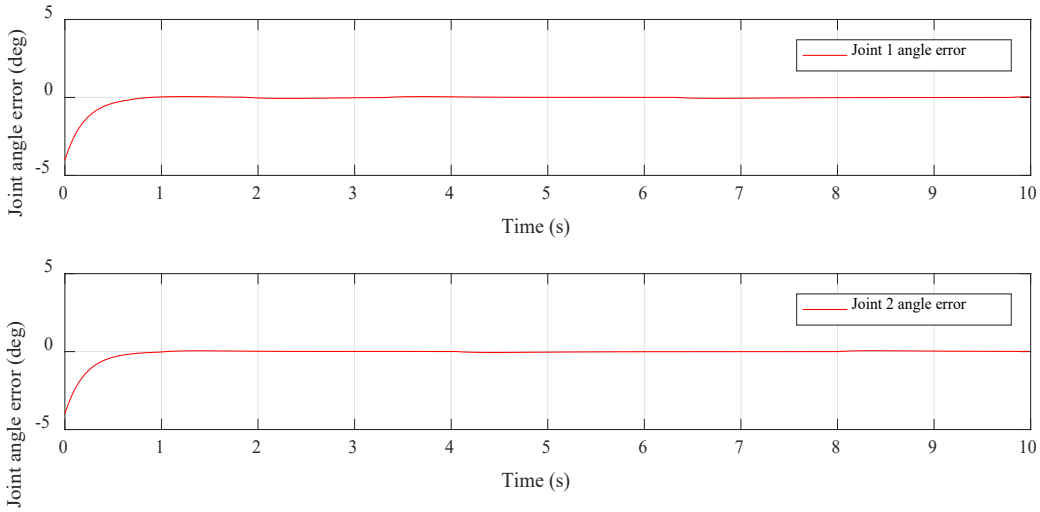

Figure 6. The position errors for link 1 and link 2

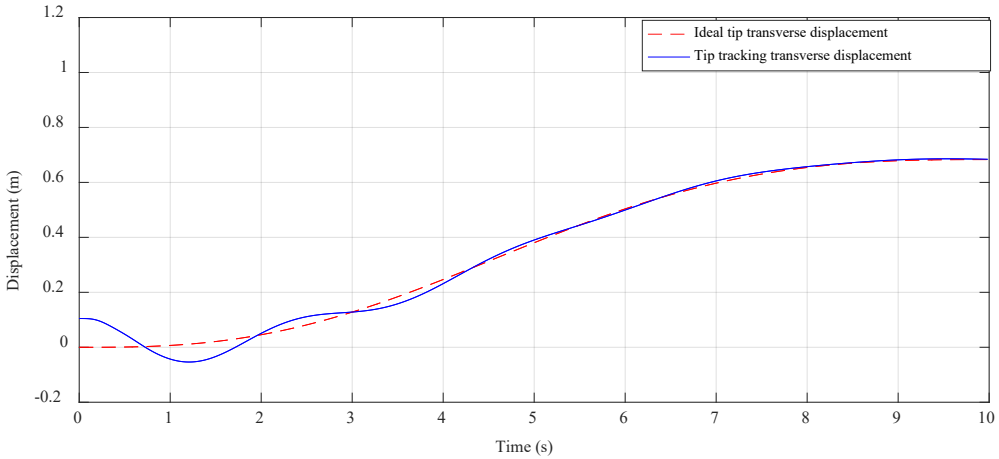

Figure 7. Ideal tip transverse and tip tracking transverse displacements.

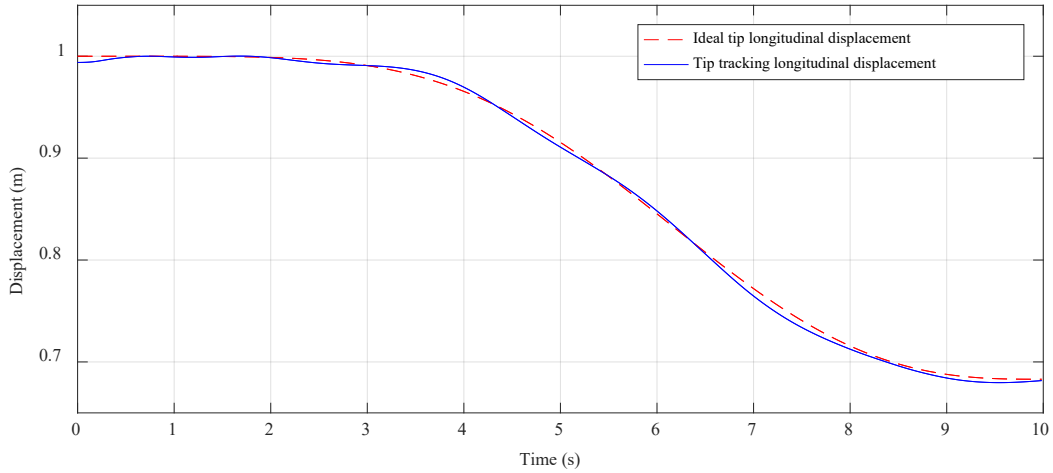

Figure 8. Ideal tip longitudinal and tip tracking longitudinal displacements.

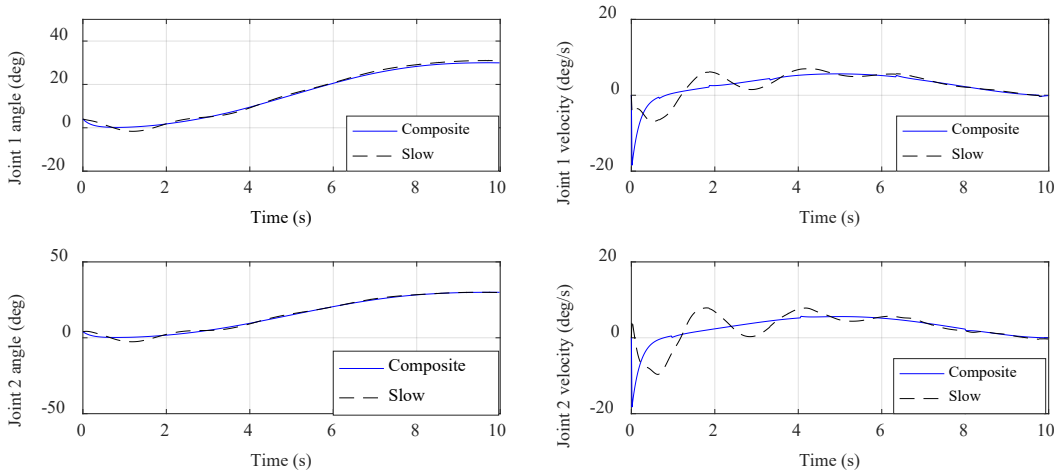

Figure 9. Joint angle 1 and joint angle 2 tracking performances.

It can be observed that adaptive robust RBF control based on global approximation deals effectively with the unknown nonlinear robot function.

5. Conclusion

In this paper, an ARBFANN control for two-flexible–link robots based on global approximation was proposed, instead of the partitioned neural network used in many papers. The approach proposed in this paper differs from the previous one as the mode shapes are derived and normalized using the generalized orthonormality relations, which results in simplified block-diagonal matrices of both links of the TFLR. The ARBFANN control guarantees the tracking of the desired trajectory while the optimal control stabilizes the vibration.

References

1. Aoutin, Y., and Chevallereau, C., The singular perturbation control of a two-flexible-link robot, *Proceedings IEEE International Conference on Robotics and Automation (ICRA)*, Atlanta. GA, pp.737-742, May 1993.
2. Borne, P., Dauphin-Tanguy, G., Richard, J. P., Rotella, F., and Zambetakis, I., *Modélisation et identification des processus*. Edit Tecnip, collection Méthodes et techniques de l'ingenieur, Paris, 1992.
3. Bryson, A. E., and Ho, Y. C., *Applied Optimal Control: Optimization, Estimation, and Control*. Wiley, New York, 1975.
4. Cai, C., Wang, Z., Xu, J., and Zou, Y., *Finite Frequency Analysis and Synthesis for Singularly Perturbed Systems*. Springer International Publishing Switzerland, 2017.
5. Chow, W. J., and Kokotovic, P. V., Two-time-scale feedback design of a class of nonlinear systems, *IEEE transactions on Automation and Control*, vol. AC-23, no. 3, pp. 438-443.
6. De Luca, A., and Siciliano, B., Closed-form dynamic model of planar multilink lightweight robots, *IEEE Transactions on Systems, Man Cybernetics SMC*, vol. 21, no. 4, pp. 826-839, 1991.
7. Feng, G., *A*., Compensating scheme for robot tracking based on neural networks. *Robotics and Autonomous Systems*, vol. 15, no. 3, pp.199-206, 1995.
8. Gee, S.S., Lee, T. H. and Tan, E. G., Adaptive Neural Network Control of Flexible Link Robots based on Singular Perturbation. *Proceedings of 1997 IEEE International Conference on Control Applications*, Hartford, CT October 5-7, 1997.
9. Kokotović, P. V., and Haddad, A. H., Controllability and Time-optimal Control of Systems with Slow and Fast modes, *IEEE Transactions on Automatic Control*, vol.20., no. 1, pp. 111-113, 1975.
10. Lewis, F. L., Jagannathan, S., and Yesilderek, A., *Neural Network Control of Robot Manipulators and Nonlinear Systems*. Taylor & Francis, inc., 325 Chestnut St Suite 800 Philadelphia, PA, United States, 1998.
11. Lewis, FL, Liu, K., and Yesilderek, A., Neural net robot controller with guaranteed tracking performance. *IEEE Transactions on Neural Networks,* vol. 6, no. 3, pp. 703-715, 1995.
12. Liu, J., *Radial Basis Function (RBF) Neural Network Control for Mechanical Systems*. Design, Analysis, and Matlab Simulation. Springer, Tsinghua University Press, 2013.
13. Moallem, M., Khorasani, K., and Patel R. V., Tip Position Tracking of Flexible Multi-Link Manipulators: An Integral Manifold Approach, *Proceedings of the 1996 IEEE International Conference on Robotics and Automation.* Minneapolis, Minnesota, April 1996.
14. Moallem, M., Khorasani, K., and Patel, R. V., An integral Manifold Approach for Tip-Position Tracking of Flexible Multi-Link Manipulators. *IEEE Transactions on Robotics and Automation,* vol. 13, no. 6, pp. 823-837, December 1997.
15. Naidu, D.S., Singular Perturbations, and Time Scales in Control Theory and Applications: An Overview. *Dynamics of Continuous, Discrete and Impulsive Systems Series B: Applications and Algorithms*, vol. 9, no. 2, pp. 233-278, 2002.
16. Rahimi, HN., and Nazemizadeh, M., Dynamic analysis and intelligent control techniques for flexible manipulators: a review, *Advanced Robotics*, vol. 28, no. 2, pp. 63-76.
17. Siciliano, B., and Book, W. J., A Singular Perturbation Approach to Control of Lightweight Flexible Manipulators, *The International Journal of Robotics Research*, vol. 7, no. 4, pp. 79-90, 1988.
18. Siciliano, B., Prasad, J. V. R., and Calise, A. J., Output Feedback Two-Time Scale Control of Multilink Flexible Arms, *Journal of Dynamic Systems, Measurement and Control*, vol.114, no. 1, pp. 70-77, 1977.
19. Subhudi, B., and Morris, A.S., Dynamic modeling, simulation and control of manipulator with flexible links and joint. *Robotics and Autonomous Systems.*41, pp.257-270, 2002.
20. Subhudi, B., and Morris, A.S., Generalised Modelling, simulation and control design for manipulators with flexible links and flexible/ rigid joints. Research report. University of Sheffield, UK., 2001.
21. Tekweme, F. K., and Nel, A., Parametric Study of Suitable Orthogonality Conditions for Planar Multilink Flexible Robots, *Proceedings of 10th South African Conference on Computational and Applied Mathematics*, pp. 503-512, 2016.

22. Tekweme, F. K., Dimensional Analysis of Natural Vibrations of Planar Multilink Flexible Robots with Elastic Constraints at Actuator Gearhead Shaft-Link Couplings. *Proceedings of the International Conference on Industrial Engineering and Operations Management. Pretoria/ Johannesburg, South Africa, October 29-November 1,* pp. 558-568, 2018c.
23. Tekweme, F. K., Dynamic Modelling and Simulation of Planar Flexible-link Robots with Rotational Restraints at the Joint-Link Couplings. *Proceedings of the 11th South African Conference on Computational and Applied Mathematics,* pp. 588-597, 2018b.
24. Tekweme, F. K., Parametric Study of Natural Frequencies and Mode Shapes of Planar Flexible-link Robots with Elastic Rotational Restraints at the Joint-Link Couplings. *Proceedings of the 11th South African Conference on Computational and Applied Mathematics*, pp. 375-385, 2018a.
25. Zhu, S. Q., Lewis, F. L., and Hunt, L. R., Robust Stabilization of the Internal Dynamics of Flexible Robots, *Proceedings of the 33rd on Decision and Control,* Lake Buena Vista, FL, 1994.

6. Bibliography

Francis Kunzi Tekweme is a senior lecturer in the Department of Mechanical Engineering at the University of Johannesburg, RSA. He holds a BEng in Mechanical Engineering from the University of Kinshasa, and a Masters and a Ding in Mechanical Engineering from the University of Johannesburg, RSA. Francis research interests include Microwave Energy Heating, Robotics, Artificial Intelligence (Machine Learning), and Programming.